

In-plane Shear Test and Application Study of Seismic Retrofit Timber Frame with CFRTP Strands

Hina Takizawa¹, Nobuji Sakurai², Yuya Takaiwa³

ABSTRACT: In this study, we conducted a static in-plane shear test of a seismic retrofitted timber frame using CFRTP strands for the purpose of clarifying the usefulness of seismic retrofitting of timber buildings using CFRTP strands. The results were analysed to clarify the deformation mechanism. Based on the results, seismic retrofitting was carried out on the actual building, and the usefulness of seismic retrofitting and the area of application of the experimental results and design method were clarified.

KEYWORDS: Timber Frame, In-Plane Shear Test, Carbon Fiber, Thermoplastic, Seismic Retrofitting

1 Introduction

Carbon fiber-reinforced materials are advanced materials used in a wide range of fields in engineering, and are also attracting attention in the field of construction [1]. Since carbon fiber composite materials have the characteristics of high strength, no rust, and no dew condensation, there are cases where they are suitable for seismic retrofitting of timber buildings instead of building steel materials [2]. In the previous study, the authors have developed an end fixing structure for CFRTP strands with toughness [3] [4] [5]. An in-plane shear test was conducted on a timber frame reinforced using CFRTP strands to clarify the in-plane shear performance. [6]. However, in the actual seismic retrofitting of timber buildings, there are cases where it is applied to a structure whose aspect ratio is different from that of the specimen, and it is not possible to adopt the same connection details as the specimen. At present, the design supervisors and contractors make decisions on a case-by-case basis at the construction site and many issues remain from the perspective of adapting to actual buildings. Therefore, we will conduct research aimed at clarifying the usefulness of seismic retrofitting of timber buildings using CFRTP strands. In order to achieve the purpose, in this report, the in-plane shear test was carried out and analyzed by adding a new specimen specification to the experimental result of the previous study [6]. Then, the in-plane shear performance and deformation mechanism were clarified, and the usefulness was clarified by conducting a trial construction test by seismic retrofitting to the actual building. Therefore, it is possible to clarify the differences that may occur when applying the specimen specifications and the actual building, and to clarify the area of application and design method of the test results. Here, most of the previous

study on the development of seismic retrofitting members for timber buildings is limited to understanding the in-plane shear performance when adapted to the specimens. On the other hand, in this study, the effectiveness is clarified not only by grasping the in-plane shear performance but also by performing adaptation verification by trial construction tests on actual buildings and that is the feature of this research.

2 In-Plane Shear Test

An in-plane shear test was performed on a timber frame reinforced with CFRTP strands to examine the possibility of adapting the CFRTP strands to the vertical surface of a timber building.

2.1 The Outline of Specimen

2.1.1 Timber Frame

Assuming a general timber house, specimen were subjected to a static in-plane shear test using a timber frame with a wall height of 2910 mm, a wall width of 910 mm, and a wall width of 1820 mm. A total of 10 specimen were tested, 5 pieces each for a specimen with a wall width of 910 mm (910 specimens) and a specimen with a wall width of 1820 mm (1820 specimens). Figure 1 and Figure 2 show the specimens diagram, and Table 1 shows elements of specimen. The specifications of the specimen are shown in Table 2 and Table 3. and compared by 5 parameters. The first is the torque value of the stainless bolt at one end of the CFRTP strand, which was controlled by hand tightening at 2Nm and 10Nm. The second is whether or not the wood (a corbel) is fixed to attach the CFRTP strand to the column. Specimen 910-3, 910-4, 910-5, 1820-1, 1820-2, 1820-3, 1820-5 were fixed in 4 places with screws. The third is the difference in the shape of the holes made in the column to penetrate CFRTP strands.

¹ Hina Takizawa, Graduate School, Dept. of Architecture, Faculty of Science and Engineering, Toyo University,

² Nobuji Sakurai, Nose Structural Corporation Co., Ltd,

³ Yuya Takaiwa, Associate Professor, Department of Architecture, Faculty of Science and Engineering, Toyo University, Dr. Eng. takaiwa@toyo.jp
2100 Kujirai, Kawagoe-shi, Saitama, Japan (350-8585)

The hole shape of specimen 910-1,910-2,910-3,1820-1,1820-2,1820-3 were circular, and the hole shape of specimens 910-4,910-5,1820-4,1820-5 are square. Figure 3 shows the fixing method of a corbel fixed with screws and the shape of the through hole of the CF RTP strand. The fourth is the presence or absence of side protrusions (protrusions of CF RTP socket) that are created when making a CF RTP socket. Specimens 910-1,910-2,910-3 and 1820 Specimen were designed to remove the protrusions of CF RTP socket, and Specimen 910-4 and 910-5 were specified to leave them. The fifth is the difference in the order when fixing the corbel of the CF RTP strand and the column. Specimen 910-1,910-2,910-3,1820-1,1820-2 and 1820-3 adjusted the torque value of the CF RTP strands after fixing the corbel to the column. Specimen 910-4,910-5,1820-4 and 1820-5 fixed the corbel to the column after tensioning the CF RTP strands.

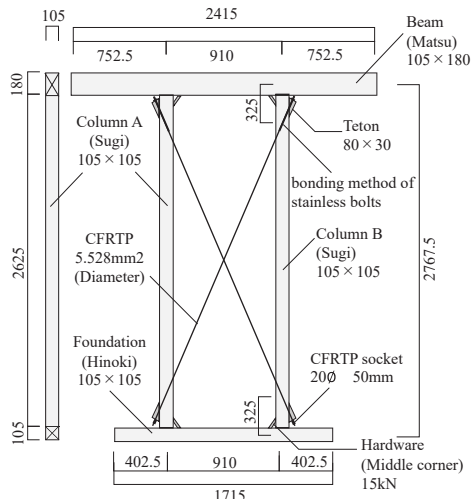


Figure 1: Specimen Diagram (910 specimen)

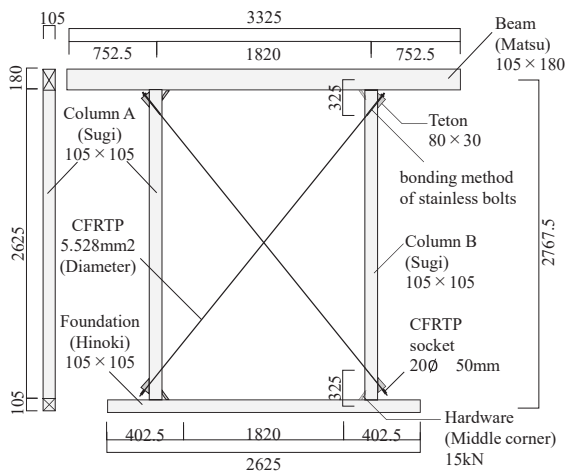


Figure 2: Specimen Diagram (1820 specimen)

Table 1: Elements of specimen

Element	Section size (mm)
Beam (Matsu)	105×180
Column (Sugi)	105×105
Foundation (Hinoki)	105×105
CF RTP	5.528(diameter)

Table 2: Details of specimen (910 specimen)

No.	The torque value	Fixing corbels	The shape of a hole of CF RTP	protrusions of CF RTP socket	Construction procedure	Diameter of CF RTP socket
910-1	10 Nm	noting	Round	Not Available	Fixing corbels ↓ tightening a bolt of CF RTP strand	20φ
910-2	2Nm	screwed				
910-3		noting	Square	Available		
910-4		screwed			tightening a bolt of CF RTP strand ↓ Fixing corbels	
910-5	noting					

Table 3: Elements of specimen (1820 specimen)

No.	The torque value	Fixing corbels	The shape of a hole of CF RTP	Protuberance of CF RTP socket	Construction procedure	Diameter of CF RTP socket
1820-1	2Nm	screwed	Round	Not Available	Fixing corbels ↓ tightening a bolt of CF RTP strand	20φ
1820-2						
1820-3		screwed	Square		Available	
1820-4		noting				tightening a bolt of CF RTP strand ↓ Fixing corbels
1820-5		screwed				

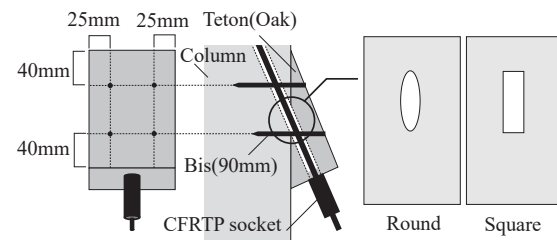


Figure 3: How to fix a corbel and The shape of hole of CF RTP

2.1.2 CF RTP strand

The CF RTP strand used in the test composed 7 twisted wires with a diameter of 2.1mm, and the cross-sectional area is 24 mm² and the tensile modulus of it is 110 kN/mm². The end fixing structure consists of two types. One side is a CF RTP socket, which is known to be ductile fracture at about 15 kN from experiments. The other side

is a bonding method of stainless bolt, which breaks brittlely with a load larger than 15 kN. Since the CFRTP socket yields before the stainless bolt, the CFRTP strand has toughness. Figure 4 shows the results of a pull-out test of a CFRTP strand suitable for this test. The test method was based on previous studies. As a result of the test, it was confirmed that the behavior of the CFRTP socket was that there was no brittle fracture even if a first yield point due to adhesive yielding, a second yielding point when the maximum yield strength was reached, and then a displacement of 40 mm occurred.

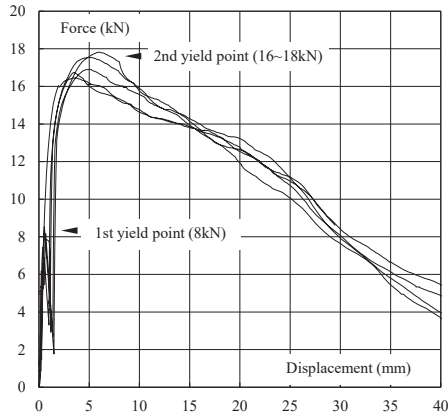


Figure 4: CFRTP socket Force-Displacement Relationship[6]

2.2 Method and measurement plan of the test

The loading device adopts a column base fixed type. It is fixed to the specimen with an in-plane restraint jig on the beam of the specimens, and the base is fixed to the specimen fixed beam. An oil jack is used to horizontally apply a positive and negative load to the specimen. In the loading cycle (repetition history), the apparent shear deformation angle of the specimen is $\pm 1/450$, $\pm 1/300$, $\pm 1/200$, $\pm 1/150$, $\pm 1/100$, $\pm 1/75$, $\pm 1/50$ rad. Deformation control is performed three times, and a positive and negative load is performed once with a deformation angle of $\pm 1/30$ rad. After that, the specimen is loaded until the maximum load is reached and the load drops ($0.8P_{max}$) or a deformation angle reaches $1/10$ rad or more. A total of 7 displacements are measured: horizontal displacement of the top of the specimen, horizontal displacement of the base of the specimen, vertical displacement of the column (2 points), horizontal displacement of the fixed beam, and vertical displacement of the jig (2 points). In addition, the strain is measured with a strain gauge at two points on the front and back of the CFRTP strands. Figure 6 and Figure 7 show respectively the displacement measurement points and strain gauge mounting positions. An in-plane shear test of a timber frame reinforced with CFRTP strands is performed to confirm the strength and fracture morphology. The shear deformation angle of the timber frame obtained by the displacement meter 1 and the displacement meter 2 was used for control.

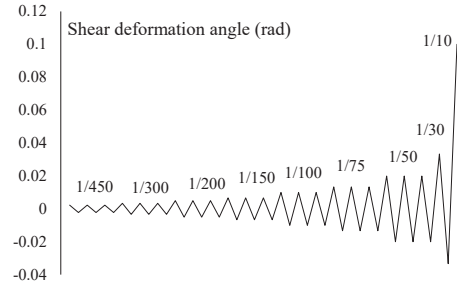


Figure 5: Repetition History

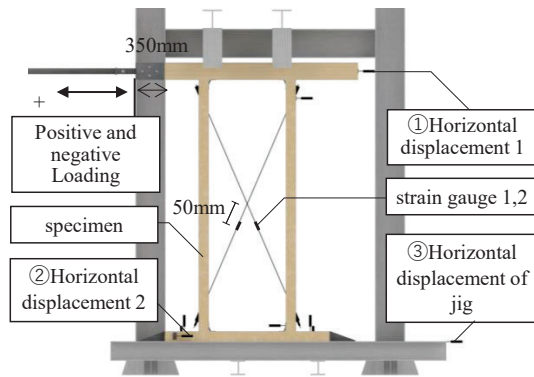


Figure 6: The Experimental Device and Specimen

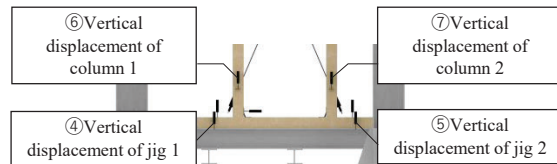
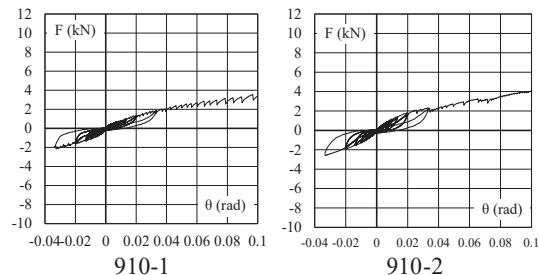


Figure 7: Points of Measurements on the Back

2.3 Result of the test

Figure 8 and Figure 9 show the relationship between the shear force (F) and the shear deformation angle (θ) of the 910 specimen and 1820 specimen, respectively. Tables 4 and 5 show the shear deformation angles of the 910 specimen and 1820 specimen at the first yield (θ_{yield}), the shear force of the timber frame at the first yield (P_{yield}), and the maximum shear force (P_{max}), respectively.



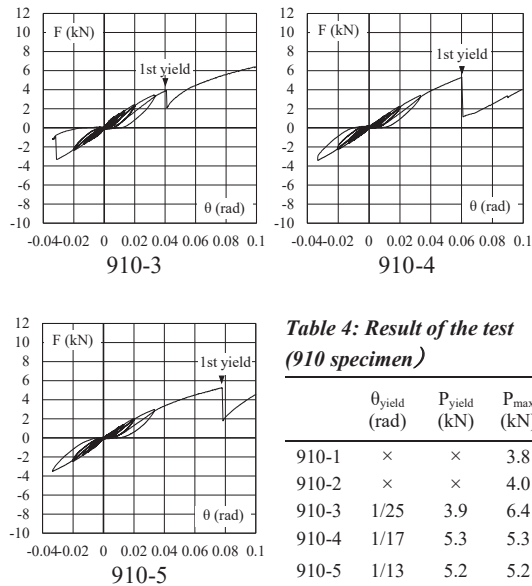


Figure 8: Shear Force-Shear Deformation Angle Relationship (910 specimen)

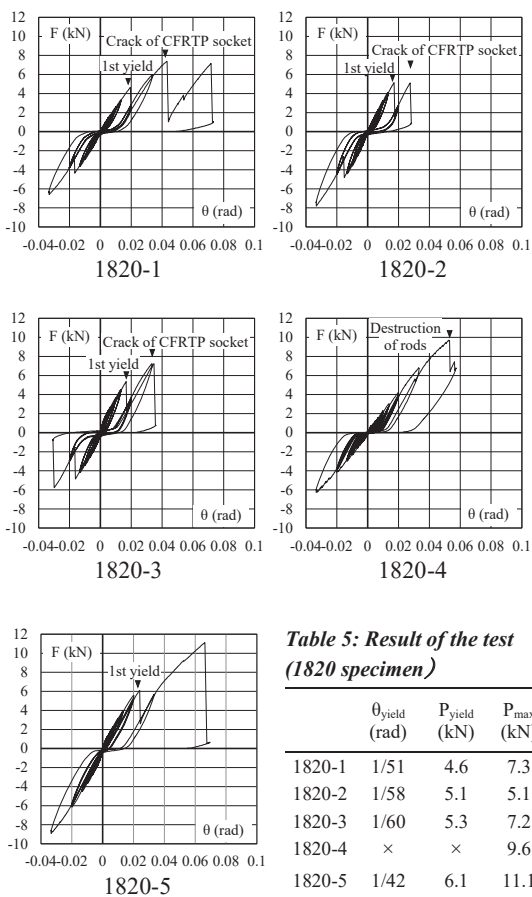


Figure 9: Shear Force-Shear Deformation Angle Relationship (1820 specimen)

Table 4: Result of the test (910 specimen)

	θ_{yield} (rad)	P_{yield} (kN)	P_{max} (kN)
910-1	×	×	3.8
910-2	×	×	4.0
910-3	1/25	3.9	6.4
910-4	1/17	5.3	5.3
910-5	1/13	5.2	5.2

2.4 Analysis

Analysis is performed based on the differences in the specifications of the specimens and the test results..

2.4.1 Torque value of stainless bolt

specimen 910-2 with a torque value of 2 Nm at one end of the CFRTP strand was compared with specimen 910-1 with a torque value of 10 Nm. Figure 10 shows the relationship between the shear deformation angle and the shear force of the specimen 910-1 and specimen 910-2. The specimen 910-1 with a large torque value had a maximum share force of 0.3 kN smaller than that of the specimen 910-2. It is considered that this is because the specimen bends inward when the torque value is large, and the force opposite to the shearing force of the timber frame is applied to it.

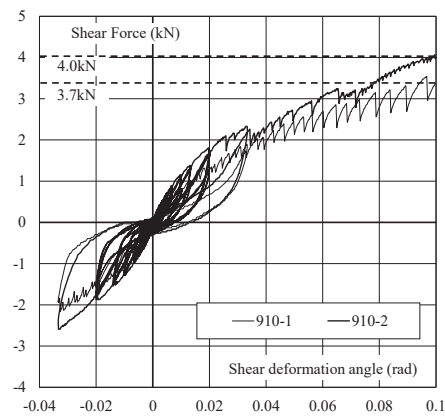


Figure 10: Shear Force-Shear Deformation Angle Relationship (910-1,910-2)

2.4.2 Fixing corbels

Specimen 910-2 and 1820-4, which allowed movement without fixing the corbels, and Specimen 910-3 and 1820-5, which had the corbels fixed with screws, were compared. Figure 11 and Figure 12 show the relationship between the shear deformation angle and the shear force of the specimen 910-2,910-3,1820-4 and 1820-5 respectively. specimen 910-2 and 1820-4 that did not fix the corbel allow the timber frame to be deformed by the corbel slipping on the column surface. Therefore, the CFRTP socket did not first yield. In the specimen 1820-4, the rod of the CFRTP strand broke. The CFRTP socket first yielded at 1/25 rad for the specimen 910-3 and 1/42 rad for the test body 1820-5 with the corbel fixed. When the corbel is not fixed, the deformation performance of the timber frame can be improved. It was confirmed that when the corbel is fixed, the maximum share force is 2.4kN for the 910 specimen 1.4kN for the 1820 specimen compared to the case where the corbel is not fixed.

Table 5: Result of the test (1820 specimen)

	θ_{yield} (rad)	P_{yield} (kN)	P_{max} (kN)
1820-1	1/51	4.6	7.3
1820-2	1/58	5.1	5.1
1820-3	1/60	5.3	7.2
1820-4	×	×	9.6
1820-5	1/42	6.1	11.1

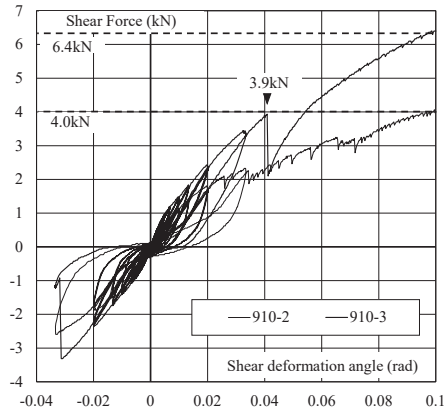


Figure 11: Shear Force-Shear Deformation Angle Relationship (910-2,910-3)

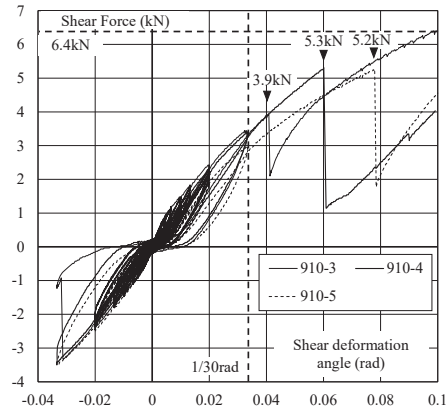


Figure 13: Shear Force-Shear Deformation Angle Relationship (910-3,910-4,910-5)

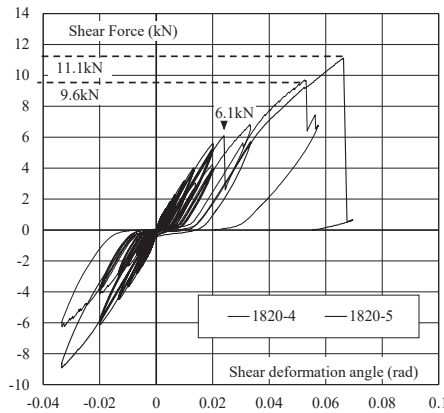


Figure 12: Shear Force-Shear Deformation Angle Relationship (1820-4,1820-5)

2.4.3 Protuberance of CFRTSP socket

Specimen 910-3 without protuberance of CFRTSP socket and specimens with it were compared with specimen 910-4 and 910-5. Figure 13 shows the relationship between the shear deformation angle and the shear force of the specimen 910-3, 910-4 and 910-5. Specimen 910-3 without protuberance of CFRTSP socket occurred first yield at $1/25$ rad, and specimen 910-4 and 910-5 with it occurred first yield at $1/17$ rad and at $1/13$ rad, respectively. The maximum shear force was 6.4 kN at the shear deformation angle of $1/10$ rad for the specimen 910-3, and 5.3 kN and 5.2 kN at the first yield for the specimen 910-4 and 910-5, respectively. If there is a protuberance of CFRTSP socket, the timber frame is given nearly twice the deformation performance of $1/30$ rad, which is the design criteria of a traditional timber building. On the other hand, when the CFRTSP socket had no protuberance of CFRTSP socket, the maximum yield strength was about 1 kN larger than that with it.

2.4.4 The shape of a hole of CFRTSP strand

Specimen 910-3, which uses a circular hole to make a CFRTSP strand through a column, and specimen 910-4 and 910-5 which have a square hole, are compared. Figure 14 shows the initial stiffness of a timber frame with a shear deformation angle of 0 rad to $1/450$ rad, and Figure 15 shows difference of embedment due to the shape of a hole of CFRTSP strand. Specimen 910-3 with circular holes for CFRTSP strands have 1.3 to 1.8 times higher initial stiffness than specimen 910-4 and 910-5 with square holes. When the shape of the hole for the CFRTSP strand is circular, it is considered that it is difficult to dig in because the contact area between the CFRTSP strand and the wood is large.

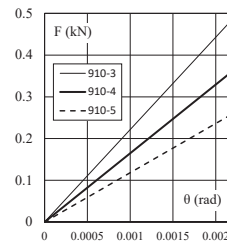


Figure 14: Initial stiffness (910-3,910-4,910-5)

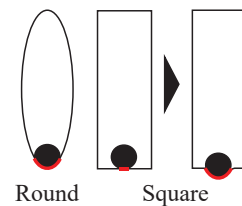


Figure 15: Difference of Embedment due to the shape of a hole of CFRTSP strand

2.4.5 Construction procedure of CFRTSP strands

The test results were compared due to the difference in the construction procedure when constructing the CFRTSP strand. Figure 16 shows the difference in the construction procedure of the CFRTSP strand. Specimen 910-3 tightened the bolt of the CFRTSP strand after fixing the corbel. On the other hand, specimen 910-4 and 910-5 fixed the corbel after tightening the bolt of the CFRTSP strand. When the receiving material of the CFRTSP strand is fixed first, the hole for the CFRTSP strand of the corbel and the column are fixed in the same position, so that the CFRTSP strand easily sinks column inside the timber frame. On the other hand, if the bolt of the CFRTSP strand is

tightened first, the position of the hole for the CFRTP strand of the corbel and the column is misaligned, so that it is easy to sink column the outside of the timber frame. The outer embedment of the timber frame has a greater contribution to the shear displacement of the timber frame than the inner.

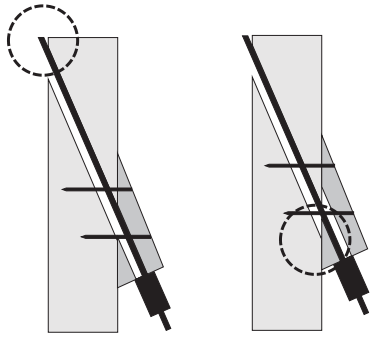


Figure 16: The Difference of Embedment of CFRTP Strand due to Construction Procedure

2.4.6 Diameter of CFRTP socket

A specimen 1820-1 using a CFRTP socket with a diameter of 20 mm and specimen 1820-5 using a CFRTP socket with a diameter of 30 mm were compared. Figure 17 shows the relationship between the shear deformation angle and the shear force of the specimen 1820-1 and 1820-5. When a CFRTP socket with a diameter of 20 mm was used, the shear force did not increase because the CFRTP socket cracked after the first yield, and the maximum shear force was 7.4 kN. On the other hand, the CFRTP socket with a diameter of 30 mm did not crack after the first yield, and the maximum shear force was 11.1 kN, which was the highest among all the specimens. By preventing the CFRTP socket from cracking, the shear force of the timber frame wall can be improved.

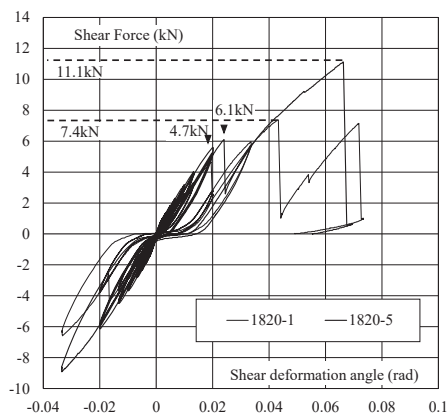


Figure 17: Shear Force-Shear Deformation Angle Relationship (1820-1,1820-5)

3 Analysis of Shear Deformation Mechanism of Specimen

3.1 The Outline of Analysis

It was analyzed how much the factors that cause shear displacement in the timber frame wall contribute to the actual shear displacement. Figure 18 shows each factor that causes shear displacement.

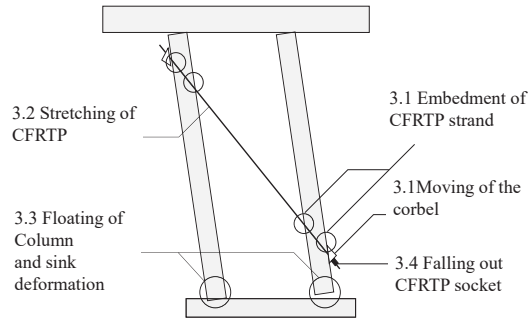


Figure 18: Factors Contributed to the Shear Deformation

3.2 How to Analyse

Using the analysis method of the factors that cause shear displacement of the timber frame proposed in the previous study [6], the contribution rate of each factor that causes shear displacement in the specimens is calculated.

3.3 The Results of Analysis

Tables 6 and Table 7 show the contribution rates of each factor that causes shear displacement of 910 specimen and 1820 specimen. In the tables, 3.1 shows Indentation deformation of CFRTP Strand and 3.2 shows axis deformation of CFRTP strand and 3.3 shows rotational deformation of the timber and 3.4 shows deformation of falling out CFRTP socket. In the 910 specimen, the shear displacements of the specimen 910-3, 910-4 and 910-5 with falling out the CFRTP socket account for about 30% of the total. In the 1820 specimen, when the CFRTP socket is fallen out, the effect on the shear displacement is larger than that in the 910 specimen. In specimen 1820-5, since all the sockets were fallen out, the shear displacement due to the sockets being fallen out was calculated to be larger than the actual one.

Table 6: Each Factor Causes the Shear Displacement (910 specimen)

	The Shear Displacement ration(%)				
	910-1	910-2	910-3	910-4	910-5
3.1	56.8	55.1	11.4	52.4	48.9
3.2	7.4	9.7	18.0	14.6	13.8
3.3	18.6	17.5	23.7	21.1	25.1
3.4	0	0	30.9	30	30.2
Total	82.8	82.4	84.2	118	118

Table 7: Each Factor Causes the Shear Displacement(1820 specimen)

	The Shear Displacement ration(%)				
	1820-1	1820-2	1820-3	1820-4	1820-5
3.1	-0.22	-5.1	-0.03	27.3	20
3.2	12.6	16	26.2	16.8	21.1
3.3	13.7	12.7	18.4	19.4	23.1
3.4	80.6	110	89.3	0	84.9
Total	106	133	134	63	149

4 Trial Construction Test by Applying to Actual Building

4.1 The Outline of the Building

The actual building, which has been seismically reinforced with CFRTP strands, is a timber building exhibited at National Museum of Ethnology. The actual building is shown in Photo 1 and Photo2, construction condition is shown in Photo 3, Adjustment of initial tension and the reinforcement drawing is shown in Figure 19.



Photo 1: View from outside of the building

Photo 2: View from inside of the building



Photo 3: Construction condition

Photo 4: Adjustment of initial tension

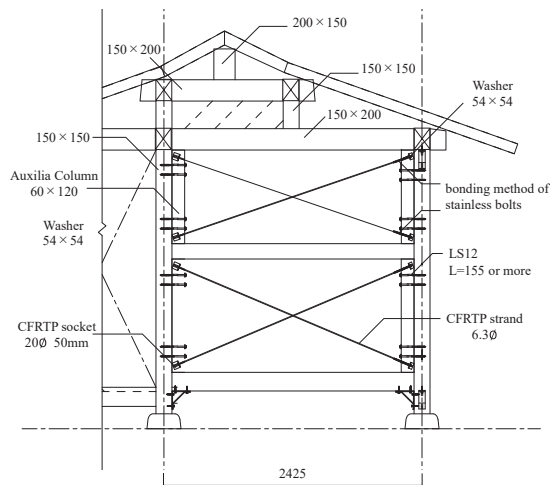


Figure 19: Drawing of Actual Building

4.2 Comparison of the Construction Status of the Specimen and the Actual Building

The construction status of the specimens and the actual building was compared. The difference between the specimens and the actual building will be described. There were the construction procedure when installing the CFRTP strand (4.3), the size of the washer installed between the CFRTP strand and the corbel (4.4), and the structural dimension of the wall reinforced by the CFRTP strand (4.5).

Table 8: The Difference specimens and actual building

		Specimens	Actual building
4.3	Construction procedure	(1) Fixing corbels ↓ Tightening a bolt of CFRTP strand (2) Tightening a bolt of CFRTP strand ↓ Fixing corbels	Fixing corbels ↓ tightening a bolt of CFRTP strand
4.4	The size of a washer (mm)	62×62	54×54
4.5	The size of a wall(mm)	(1)910×2767.5 (2)1820×2767.5	case-by-case

4.3 Impact of Construction Procedure

When constructing a real building, first tighten the bolts of the CFRTP strand and then fix the corbel. Therefore, it is considered that the CFRTP strands are easily sunk on the outside of the timber frame, and the deformation performance of timber frame is improved.

4.4 Impact of The Size of a Washer

A washer is installed between the CFRTP strand and the corbel. A washer of 62 mm x 62 mm was used in specimen, but a washer of 54 mm x 54 mm was used in the actual building. Using the formula (1), it was confirmed whether or not the washer would be dented due to the smaller washer. The allowable bearing stress is 23.3 kN. Since the axial force that can be borne by the CFRTP strand is 15 kN, it was confirmed that the washer does not sink into the corbel until the CFRTP strand breaks.

$$F_{cv} \times \frac{2}{3} \times A \quad (1)$$

F_{cv} : Basic strength of bearing (12N/mm) [7]
A: The area of a washer(2910mm²)

4.5 Impact of Aspect Ratio of the Timber Frame

In order to obtain the change in the stiffness of the timber frame due to the change in the aspect ratio of the wall, it was verified using the formulas (2) to (5). The change in

the stiffness of 910 specimen to 1820 specimen is considered to be influenced by the change in the aspect ratio of the timber frame and the change in the stiffness of the CFRTP strand. First, the effect of the change in the stiffness of the CFRTP strand is removed from the change in the stiffness of the wall.

$$\frac{P_{1820}}{P_{910}} \div \frac{L_{b910}}{L_{b1820}} \quad (2)$$

P_{910} : Shear force at a shear deformation angle of 1/30 rad in 910 specimen (3.37kN)

P_{1820} : Shear force at a shear deformation angle of 1/30 rad in 1820 specimen (6.59kN)

L_{b910} : Length of CFRTP Strand of 910 Specimen (2304mm)

L_{b1820} : Length of CFRTP Strand of 1820 Specimen (2792mm)

The effect of wall stiffness due to changes in the aspect ratio of the wall of the actual building is shown in the formula (3).

$$K = k_{910} \times \frac{P_{1820}}{P_{910}} \div \frac{L_{b910}}{L_{b1820}} \div \frac{W_{1820}/H_{1820}}{W_{910}/H_{910}} \times \frac{W'/H'}{W_{910}/H_{910}} \quad (3)$$

K : Stiffness of actual building wall affected by changes in wall aspect ratio

W_{910} : Width of 910 specimen (910mm)

W_{1820} : Width of 1820 specimen (1820mm)

W' : Width of the wall of actual building (2425mm)

H_{910} : Height of 910 specimen (2767.5mm)

H_{1820} : Height of 1820 specimen (2767.5mm)

H' : Height of the wall of actual building (1224.9mm)

The effect of the change in the stiffness of the CFRTP strand on the stiffness of the wall is added to the formula (3).

$$k' = K \times \frac{L_{b910}}{L_{b'}} \quad (4)$$

k' : Stiffness of the wall of actual building

$L_{b'}$: Length of CFRTP Strand of the wall of actual building (2530mm)

The axial force borne by the CFRTP strand is calculated using the wall stiffness calculated by the formula (4).

$$k' \times \frac{H'}{30} \times \frac{L_{b'}}{W'} \quad (5)$$

When an example of the wall of an actual building is calculated using the formulas (2) to (5), the stiffness of the wall is 0.23 kN / mm, and the axial force borne by the CFRTP strand is estimated to be 9.6 kN. This is less than the axial force (15 kN) that the CFRTP strand can bear and is designed within the area of application of the experimental results.

Table 9: Impact of Aspect Ratio of the Timber Frame

	910 Specimen	1820 Specimen	Actual Building
W /mm	$\frac{W_{910}}{H_{910}}$	$\frac{W_{1820}}{H_{1820}}$	$\frac{W'}{H'}$
L_b /mm	$\sqrt{W_{910}^2 + (H_{910} - 2a)^2}$ (= L_{b910})	$\sqrt{W_{1820}^2 + (H_{1820} - 2a)^2}$ (= L_{b1820})	$\sqrt{(W')^2 + (H' - 2a')^2}$ (= L_b')
k_b /kN/m	$\frac{E \cdot A}{L_{b910}}$	$\frac{E \cdot A}{L_{b1820}}$	$\frac{E \cdot A}{L_b'}$
P /kN	3.378 (= P_{910})	6.281 (= P_{1820})	$\frac{k_{1820} \times L_{1820} \times L_{b910} \times D' \times H_{1820}}{L_{910} \times L_b' \times H' \times D_{1820}} \times \frac{H'}{30}$
k /kN/m	$P_{910} \times \frac{30}{H_{910}}$	$P_{1820} \times \frac{30}{H_{1820}}$	$\frac{k_{1820} \times L_{1820} \times L_{b910} \times D' \times H_{1820}}{L_{910} \times L_b' \times H' \times D_{1820}}$

W : Width of the wall

H : height of the wall

L_b : Length of CFRTP strand

k_b : Stiffness of CFRTP strand

P : Shear force at a shear deformation angle of 1/30 rad

k : Stiffness of the wall

5 Conclusion

A static in-plane shear test of a seismic retrofitted timber frame using CFRTP strands revealed the following.

- (1) The initial tension of the CFRTP strand was examined using 910specimen. As a result, it was confirmed that when the torque value was changed from 2Nm to 10Nm, the shear force borne by the wall was reduced due to the initial deformation of the timber frame bending inward.
- (2) It was confirmed that the stiffness of the timber frame in 910 specimen changes depending on whether or not the corbel of the CFRTP strand is fixed. It was clarified that when the corbel is not fixed, the corbel allows the sliding movement on the contact surface of the column and increases the shear deformation of timber frame.
- (3) It was confirmed that the initial stiffness is affected when the shape of the hole for the CFRTP strand is different. It is presumed that this is because when the shape of the hole is circular, the contact area between the CFRTP strand and the timber is larger than when the shape of the hole is square, so it is less likely to be dented.
- (4) It was confirmed that the deformation performance of the timber frame changes depending on the construction procedure of the CFRTP strand. It is clear that the procedure of tightening the bolts and then fixing the corbel has a larger shear displacement due to the digging of the columns of the CFRTP strand than the procedure of tightening the bolts of the CFRTP strand after fixing the corbel of the CFRTP strand.

Based on the findings mentioned above, we conducted an adaptation verification by construction experiments on

seismic retrofitting actual buildings using CFRTP strands. As a result, it was confirmed that seismic retrofitting is useful by considering the influence even if the specifications are different from the specimens. In this study, the effect of changing the aspect ratio of the wall was estimated using geometry, but experimental values that can verify the aspect ratio have not been obtained. In the future, in-plane shear test will need to be conducted to clarify the effects.

ACKNOWLEDGEMENT

This work was supported by JST COI Grant Number JPMJCE1315.

REFERENCES

- [1] Kiyoshi Uzawa , Yoshihiro Saito , Atsushi Hokura : APPLICATION OF COMPOSITE MATERIALS TO CIVIL ENGINEERING AND CONSTRUCTION FIELDS -NEW INITIATIVES THROUGH ADVANCED MATERIALS AND INNOVATIVE MANUFACTURING TECHNOLOGY-, Journal of Japan Society of Civil Engineers, Ser. A1 (Structural Engineering & Earthquake Engineering (SE/EE)) 73(5), II_1-II_9, 2017.5
- [2] Yuya Takaiwa, Akina Furuie, Nobuji Sakurai, Koji Kubo, Kiyoshi Uzawa: STRUCTURAL PERFORMANCE EVALUATION OF TIMBER ARCHITECTURE WITH SEISMIC RETROFIT BY CFRTP, World Conference on Timber Engineering 2020 TA0706 2021.8
- [3] Yuya Takaiwa, Katsuhiko Nunotani, Kiyoshi Uzawa : DEVELOPMENT AND RESEARCH OF END FIXING STRUCTURE FOR EXPANDING THE USE OF CFRP STRANDS, AIJ Journal of Technology and Design 28(68), pp.36-41, 2022.2
- [4] Yuya Takaiwa, Katsuhiko Nunotani, Kiyoshi Uzawa : Development of tough CFRP strand end fixation, AIJ Journal of Technology and Design 27(65), pp.108-113, 2021.2
- [5] Yuya Takaiwa, Katsuhiko Nunotani, Atsushi Hokura, Shiro Noguchi, Nobuaki Inui, Tadashi Sakuma, Kiyoshi Uzawa: INFLUENCE OF WELDING TEMPERATURE ON ADHESION PERFORMANCE OF CFRTP STRAND ROD-SOCKET, 16th Japan International SAMPE Symposium & Exhibition 3A-06 2019.9
- [6] Hina Takizawa, Hiroki Matsumoto, Nobuji Sakurai, Kiyoshi Uzawa, Yuya Takaiwa: Structural Performance Evaluation of Timber Frame with CFRTP Reinforcement, 17th Japan International SAMPE Symposium & Exhibition S01 2021.12
- [7] Architectural Institute of Japan: Fundamental Theory of Timber Engineering, Architectural Institute of Japan, 2010.10, p.98